ACI STRUCTURAL JOURNAL TECHNICAL PAPER

Title No. 113-S21

# Discrete Shear Strength of Two- and Seven-Circular-Hoop and Spiral Transverse Reinforcement

by Yu-Chen Ou and Si-Huy Ngo

*This study developed discrete computational shear strength (DCSS) models for two-circular-hoop, two-spiral, seven-circular-hoop, and seven-spiral transverse reinforcement for reinforced concrete columns. The DCSS models show that as a shear crack moves along the column, the reinforcement shear strength varies periodically. The critical shear crack, which yields the smallest shear strength, can be from any of the shear cracks that intercept at least one edge of a hoop series or spiral. The conditions are presented for when a shear crack intercepts the two edges of every hoop series or spiral, which leads to a drastic reduction in shear strength. At the critical shear crack condition, the DCSS models yield shear strength lower than the integral averaging method. To control the error of the integral averaging method, the ratio of the reinforcement spacing to hoop or spiral diameter should be limited. Charts to correct the error are presented for use in practice.*

**Keywords:** discrete computation; integral averaging method; multi-circular-hoop transverse reinforcement; multi-spiral transverse reinforcement; shear reinforcement.

## INTRODUCTION

Circular-hoop or spiral transverse reinforcement is well-known for its better confinement effectiveness and restraint for longitudinal bar buckling than rectilinear hoop or tie transverse reinforcement. Circular-hoop or spiral reinforcement can effectively resist concrete expansion and longitudinal bar buckling by developing hoop tension at any location along hoop or spiral perimeter, whereas rectilinear hoop or tie reinforcement is only effective at corners or bends. Circular-hoop or spiral reinforcement has been extended to oblong columns (Fig. 1(a)) in the form of two interlocking hoops or spirals. Results of previous studies have shown that even with a less amount of transverse reinforcement, two-spiral oblong columns (Fig. 1(a)) have better seismic performance than conventional tied columns.[1-6] Two-spiral reinforcement has been applied in the Fujikawa Bridge columns in Japan.[4] The $P_4$ column of the bridge has an oblong cross-sectional shape with a dimension of 8500 x 6000 mm (335 x 236 in.). Each of the two spirals of the column has a diameter of 6000 mm (236 in.) and was fabricated with D32 (No. 10) bars. To reduce the size of spirals in large oblong columns such as the Fujikawa Bridge column to relieve the difficulty associated with fabrication of large spirals, innovative seven-spiral reinforcement (Fig. 1(b)) has been proposed.[7,8] Test results have demonstrated that seven-spiral reinforcement is more efficient in providing shear strength compared with two-spiral reinforcement (Fig. 1(a)) and tie reinforcement.[7] Moreover, seven-spiral columns, even with a less amount of transverse reinforcement, possess higher ductility capacity than comparable tied columns.[8]

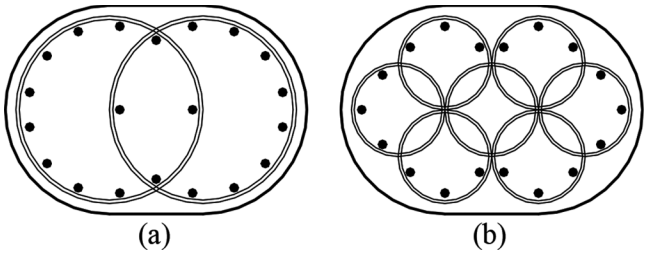


*Fig. 1—(a) Two-circular-hoop or two-spiral reinforcement; and (b) seven-circular-hoop or seven-spiral reinforcement.*

For single- and multi-circular-hoop or spiral transverse reinforcement, Caltrans SDC[9] and AASHTO[10] employ Eq. (1) to calculate shear strength provided by transverse reinforcement.

$$V_s = \frac{A_v f_{yh} D'}{s}, \text{ where } A_v = n\left(\frac{\pi}{2}\right) A_{sh} \tag{1}$$

Equation (1) was first discussed by Ang et al.[11] and Tanaka and Park[1] for single-spiral and two-spiral columns, respectively, and can be derived as follows. Assuming transverse reinforcement yields at the ultimate condition of shear, shear resistance provided by the *i*-th hoop of a hoop series (for example, Fig. 2(a), which has two hoop series) or by the *i*-th level of a spiral (for example, Fig. 2(b), which has two spirals) intersected by a shear crack is $T_{si} = A_{sh} f_{yh} (\sin\alpha_i^1 + \sin\alpha_i^2)\sin\beta$. The total shear resistance provided by all the levels intercepted by the crack is

$$\begin{aligned} V_s &= \sum_i T_{si} = \sum_i A_{sh} f_{yh} (\sin\alpha_i^1 + \sin\alpha_i^2)\sin\beta \\ &= A_{sh} f_{yh} \sin\beta \sum_i (\sin\alpha_i^1 + \sin\alpha_i^2) \end{aligned} \tag{2}$$

Assuming the spacing of transverse reinforcement is very small, a hoop series or spiral is intersected by a shear crack at a great number of locations such that within the range of $\alpha_i^1$ and $\alpha_i^2$—that is, 0 – π (Fig. 2)—$\sum_i \sin\alpha_i^1$ and $\sum_i \sin\alpha_i^2$ can each be approximated by $\sum_i \pi/4$, in which π/4 is the average value of a sine curve from 0 – π. Moreover, because the pitch is very small, β ≈ 90 degrees for spiral reinforcement. Note that β is 90 degrees for circular-hoop reinforce-

*ACI Structural Journal*, V. 113, No. 2, March-April 2016.
MS No. S-2014-291.R1, doi: 10.14359/51688058, was received April 27, 2015, and reviewed under Institute publication policies. 

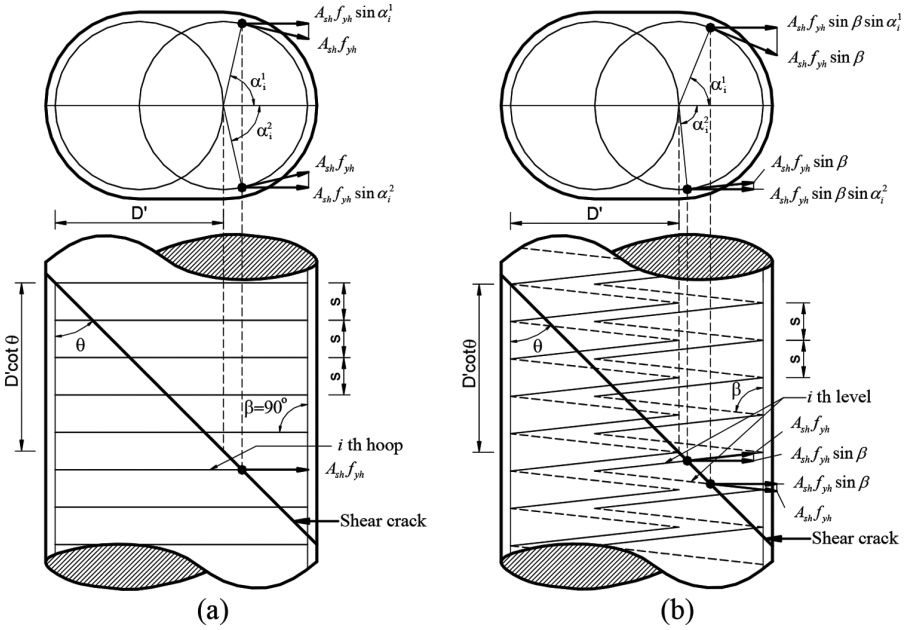


*Fig. 2—(a) Two-circular-hoop column; and (b) two-spiral column.*

ment regardless of the spacing. Therefore, sinβ in Eq. (2) equals 1. Hence, Eq. (2) becomes

$$V_s = A_{sh} f_{yh} \sin\beta \sum_i (\sin\alpha_i^1 + \sin\alpha_i^2) = A_{sh} f_{yh} \cdot 1 \cdot \sum_i \left(\frac{\pi}{4} + \frac{\pi}{4}\right) = A_{sh} f_{yh} \sum_i \left(\frac{\pi}{2}\right) \quad (3)$$

Also due to the small spacing assumption, the number of levels of a hoop series or spiral intercepted by a shear crack, which in reality is a discrete (integer) number, is approximated by the ratio of the vertical projection of the portion of the crack crossing a hoop series or spiral ($D'\cot\theta$) to the vertical spacing of the hoop series or spiral ($s$), $D'\cot\theta/s$ (Fig. 2). Hence, $n$ hoop series or spirals result in a total shear resistance of

$$V_s = A_{sh} f_{yh} \sum_i \left(\frac{\pi}{2}\right) = A_{sh} f_{yh} \left(n \frac{D' \cot\theta}{s}\right) \frac{\pi}{2} \quad (4)$$

which, with θ = 45 degrees, becomes Eq. (1). Equation (4) is referred to as integral averaging method herein.

To investigate the error associated with the small spacing assumption used in the integral averaging method (Eq. (4)), discrete computational shear strength (DCSS) models that aim to discretely compute shear strength contributed by each intersection between a shear crack and reinforcement have been studied. Dancygier[12] derived a DCSS model for single-circular-hoop reinforcement and found that the integral averaging method yielded results that were more than 10% unconservative when $s/(D'\cot\theta) \geq 0.25$. Kim and Mander[13] simplified Dancygier's model by considering the critical shear crack that produced the smallest shear strength. In addition, Kim and Mander[13] developed a DCSS model for single-spiral reinforcement and assumed β equals 90 degrees. By comparing the results of the developed DCSS models and the integral averaging method, Kim and Mander suggested that when $s/(D'\cot\theta) \geq 0.2$, the results of the integral averaging method should be modified by correction factors to limit probable unconservativeness to be less than 10%. Jaafar[14] used discrete computation to examine the error of the integral averaging method for single-spiral reinforcement and two-spiral reinforcement under strong axis bending and concluded that the error increased with increasing spiral spacing ($s$) and shear crack angle (θ). Note that in Jaafar's discrete computation, analytical representations for locations where a shear crack intercepts spiral reinforcement still need to be developed.

The objective of this study is to develop DCSS models for two- and seven-circular-hoop, and two- and seven-spiral transverse reinforcement under weak and strong axis bending. With the developed models, the error of the integral averaging method (Eq. (4)) for such types of reinforcement is examined.

## RESEARCH SIGNIFICANCE

It is the current practice to use the integral averaging method to calculate the shear strength of multi-circular-hoop and multi-spiral transverse reinforcement. However, for two- and seven-circular-hoop and spiral reinforcement, the error of the method has not received much attention in the literature. This study developed DCSS models for two- and seven-circular-hoop and spiral transverse reinforcement under strong and weak axis bending to examine the error of the integral averaging method and to provide tools for engineers to calculate the shear strength of such types of reinforcement when the error is significant.

## PROPOSED DCSS MODELS

DCSS models for single-circular-hoop and single-spiral reinforcement are derived first in this section using a new, coordinate-based approach. The models are then extended to develop DCSS models for two- and seven-circular-hoop, and two- and seven-spiral reinforcement.

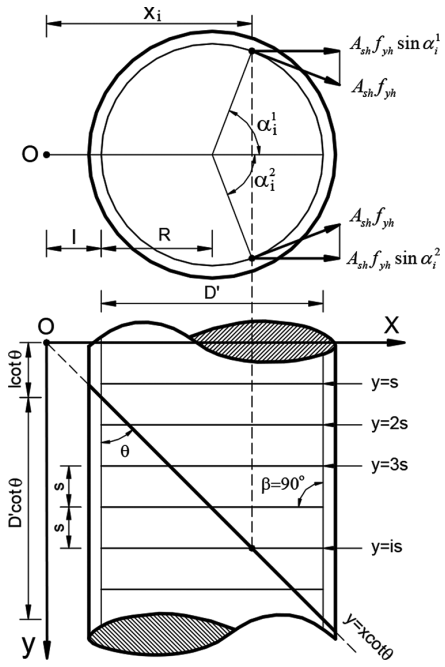


*Fig. 3—Cartesian coordinate system for single-circular-hoop reinforcement.*

## DCSS model for single-circular-hoop reinforcement

A Cartesian coordinate system is used to facilitate derivation of the DCSS model for single-circular-hoop reinforcement. As shown in Fig. 3, the origin of the coordinate system is set in the horizontal x-direction at an arbitrary distance $l$ from the edge of reinforcement and in the y-direction (vertical) is at the level of an arbitrary hoop. A shear crack with an angle θ to the longitudinal axis of the column is placed in the coordinate system so that the extension of the crack passes through the origin. Note that by changing the value of $l$, the crack can be set to start at any location along the left edge of the reinforcement. Based on the coordinate system, the shear crack can be represented by a function, $y = x\cot\theta$. The $i$-th hoop intersected by the shear crack can be represented by $y = i \cdot s$. Therefore, the x-coordinate of the intersection of the $i$-th hoop and the shear crack is

$$x_i = is\tan\theta \text{ from } \begin{cases} y = x\cot\theta \\ y = i\cdot s \end{cases} \tag{5}$$

The value of $x_i$ is bounded between the left and right edges of the reinforcement.

$$l \le x_i \le l + D' \tag{6}$$

Combining Eq. (5) and (6), the value of $i$ is bounded as follows

$$\frac{l\cot\theta}{s} \le i \le \frac{l\cot\theta}{s} + N \tag{7}$$

where $i$ is an integer, numbering the hoops; and $N = D'\cot\theta/s$, representing the ratio of the projection of the shear crack along the y-axis to the spacing of the hoops. From Fig. 3 and trigonometry, $\sin\alpha_i^1$ and $\alpha_i^2$ of Eq. (2) can be expressed by the following equation. Note that $x_i = is\tan\theta$ from Eq. (5) and $N = D'\cot\theta/s = 2R\cot\theta/s$.

$$\begin{aligned}\sin\alpha_i^1 = \sin\alpha_i^2 &= \sqrt{1-\cos^2\alpha_i} = \sqrt{1-\left(\frac{x_i - l - R}{R}\right)^2} \\ &= \sqrt{1-\left(\frac{0.5N + l\cot\theta/s - i}{0.5N}\right)^2}\end{aligned} \tag{8}$$

Substituting the previous equation into $T_{si}$ of Eq. (2) and noting that β = 90 degrees for a hoop, the shear resistance provided by the $i$-th hoop can be expressed as

$$T_{si} = 2A_{sh}f_{yh}\sqrt{1-\left(\frac{0.5N + l\cot\theta/s - i}{0.5N}\right)^2} \tag{9}$$

The total shear resistance provided by all the hoops intersected by the shear crack is

$$V_{s\_l}^{one} = \sum_i T_{si} = 2A_{sh}f_{yh}\sum_{i=\text{int}[l\cot\theta/s]+1}^{\text{int}[N+l\cot\theta/s]}\sqrt{1-\left(\frac{0.5N + l\cot\theta/s - i}{0.5N}\right)^2} \tag{10}$$

where the range of $i$ is based on Eq. (7). Equation (10) is the DCSS model for single-circular-hoop reinforcement and is applicable to any shear crack location (by adjusting $l$), and to any shear crack angle (by adjusting θ). Equation (10) is the same as Dancygier's model,[12] even though they appear to be different.

## DCSS model for single-spiral reinforcement

Similar to single-circular-hoop reinforcement, a Cartesian coordinate system is set such that the X-axis passes through the left edge of spiral reinforcement and the distance between the system origin and spiral edge is $l$ (Fig. 4). In Fig. 4, the spiral reinforcement is drawn with dashed and solid lines, representing half of the spiral on the back side of the column and that on its front side, respectively. Based on the coordinate system, the equation for the back side spiral line of the $i$-th spiral level is

$$y = \frac{s}{2D'}x + s\left(i - \frac{l}{2D'}\right) \tag{11}$$

The equation for the front side spiral line of the $i$-th spiral level is

$$y = -\frac{s}{2D'}x + s\left(i + 1 + \frac{l}{2D'}\right) \tag{12}$$

A shear crack is assumed with its extension passing through the origin of the coordinate system (Fig. 4) and can be expressed by $y = x\cot\theta$. The x-coordinate of the intersection between the crack and the back side spiral line of the

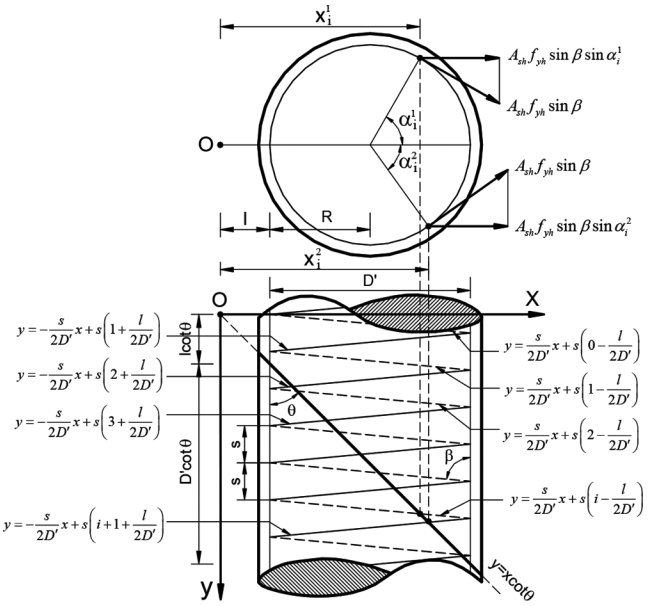


*Fig. 4—Cartesian coordinate system for single-spiral reinforcement.*

*i*-th spiral level can be derived by solving the equations of the crack line and back side spiral line.

$$x_i^1 = \frac{s(i-b)}{a_1} \text{ from } \begin{cases} y = x\cot\theta \\ y = \dfrac{s}{2D'}x + s\left(i - \dfrac{l}{2D'}\right) \end{cases} \quad (13)$$

where $b = l/2D'$ and $a_1 = \cot\theta - s/2D'$. The $x_i^1$ has the following range (from the left edge to right edge of the spiral).

$$l \le x_i^1 \le D' + l \quad (14)$$

Substituting Eq. (13) into Eq. (14) and solving for the range of *i* gives

$$\frac{l\cot\theta}{s} \le i \le N + \frac{l\cot\theta}{s} - 0.5 \quad (15)$$

where *i* is an integer, numbering the spiral level. With trigonometry and Eq. (13), $\sin\alpha_i^1$ of Eq. (2) for single-spiral reinforcement can be expressed as

$$\sin\alpha_i^1 = \sqrt{1-\cos^2\alpha_i^1} = \sqrt{1-\left(\frac{l+R-x_i^1}{R}\right)^2} = \sqrt{1-\left(\frac{0.5N + \dfrac{l\cot\theta}{s} - \dfrac{i-b}{a_1}\cot\theta}{0.5N}\right)^2} \quad (16)$$

Similarly, the x-coordinate of the intersection between the shear crack and the front side spiral line of the *i*-th spiral level is

$$x_i^2 = \frac{s(i+1+b)}{a_2} \text{ from } \begin{cases} y = x\cot\theta \\ y = -\dfrac{s}{2D'}x + s\left(i+1+\dfrac{l}{2D'}\right) \end{cases} \quad (17)$$

where $a_2 = \cot\theta + s/2D'$. The $x_i^2$ has the same range as $x_i^1$ (Eq. (14)).

$$l \le x_i^2 \le D' + l \quad (18)$$

Substituting Eq. (17) into Eq. (18) and solving for the range of *i* gives

$$\frac{l\cot\theta}{s} - 1 \le i \le N + \frac{l\cot\theta}{s} - 0.5 \quad (19)$$

Using the same procedure as in deriving $\sin\alpha_i^1$ (Eq. (16)), $\sin\alpha_i^2$ can be expressed as

$$\sin\alpha_i^2 = \sqrt{1-\left(\frac{0.5N + \dfrac{l\cot\theta}{s} - \dfrac{i+1+b}{a_2}\cot\theta}{0.5N}\right)^2} \quad (20)$$

The shear resistance provided from the back and front side spiral lines of the *i*-th spiral level can be obtained with Eq. (2) with $\sin\alpha_i^1$ and $\sin\alpha_i^2$ calculated by Eq. (16) and (20), respectively. Summing the shear resistances from all intersection points yields the total shear resistance.

$$V_{s\_l}^{one} = \sum_i T_{si} = \sum_i A_{sh} f_{yh}\left(\sin\alpha_i^1 + \sin\alpha_i^2\right)\sin\beta = A_{sh} f_{yh}\sin\beta\left[\sum_{i=\text{int}[l\cot\theta/s]+1}^{\text{int}[N+l\cot\theta/s-0.5]} \sqrt{1-\left(\frac{0.5N + \dfrac{l\cot\theta}{s} - \dfrac{i-b}{a_1}\cot\theta}{0.5N}\right)^2} + \sum_{i=\text{int}[l\cot\theta/s]}^{\text{int}[N+l\cot\theta/s-0.5]} \sqrt{1-\left(\frac{0.5N + \dfrac{l\cot\theta}{s} - \dfrac{i+1+b}{a_2}\cot\theta}{0.5N}\right)^2}\right] \quad (21)$$

where the ranges of *i* for $\sin\alpha_i^1$ and that for $\sin\alpha_i^2$ are based on Eq. (15) and (19), respectively. Equation (21) is the DCSS model for single-spiral reinforcement and is applicable to any shear crack location (by adjusting *l*), and to any shear crack angle (by adjusting θ). The Kim and Mander model[13] for single-spiral reinforcement is the same as Eq. (21) without sinβ and with $l = 0$. Note that it is necessary to include the effect of *l* (crack location) in Eq. (21) to allow Eq. (21) to be extended to two- and seven-spiral reinforcement.

### DCSS models for two- and seven-circular-hoop and two- and seven-spiral reinforcement

The DCSS models for two- and seven-circular-hoop and two- and seven-spiral reinforcement can be derived based on Eq. (10) and (21), respectively. For two-circular-hoop or two-spiral reinforcement under weak axis bending (Fig. 5(a)), because the two circular-hoop series or two spirals have the same distance from the origin of the coordinate system, the DCSS model is simply twice that of single-circular-hoop (Eq. (10)) or single-spiral (Eq. (21)) reinforcement.

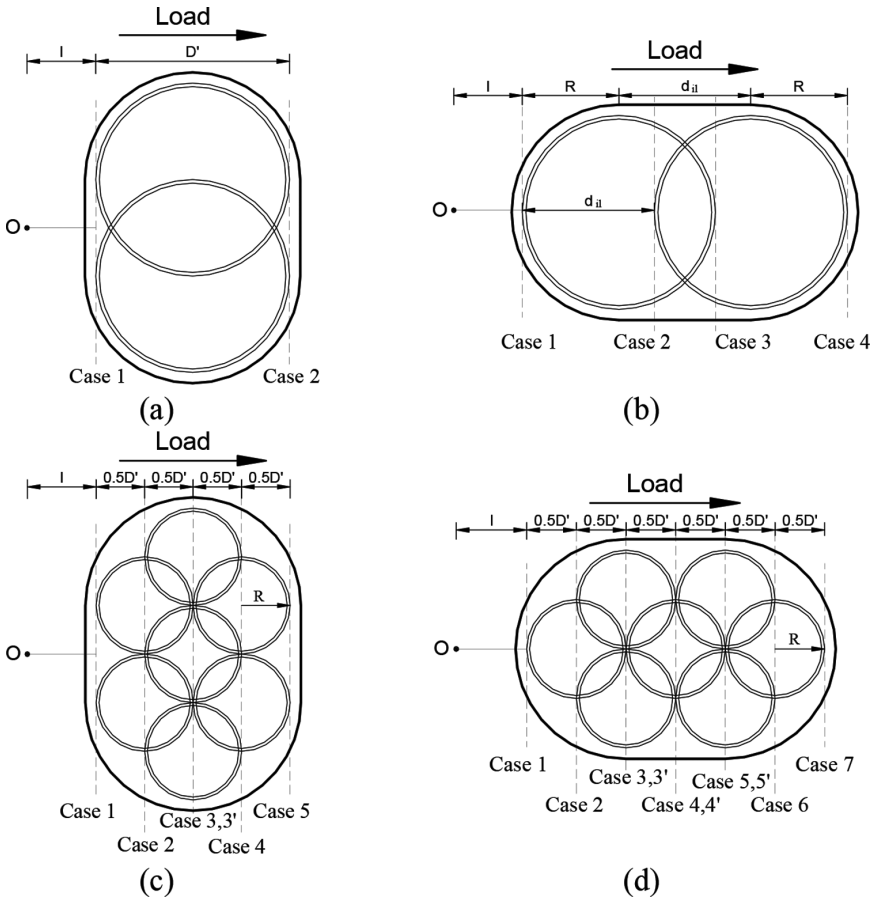


*Fig. 5—Distance from hoop or spiral edge to original of coordinate system and potential critical crack locations for: (a) two-circular-hoop and spiral reinforcement under weak axis bending; (b) two-circular-hoop and spiral reinforcement under strong axis bending; (c) seven-circular-hoop and spiral reinforcement under weak axis bending; and (d) seven-circular-hoop and spiral reinforcement under strong axis bending.*

$$V_{s\_l}^{two\_weak} = 2V_{s\_l}^{one} \tag{22}$$

For two-circular-hoop or two-spiral reinforcement under strong axis bending (Fig. 5(b)), the DCSS model is the superposition of two DCSS models for single-circular-hoop (Eq. (10)) or single-spiral (Eq. (21)) reinforcement with $l = l$ and with $l = l + d_{il}$.

$$V_{s\_l}^{two\_strong} = V_{s\_l}^{one} + V_{s\_l+d_{il}}^{one} \tag{23}$$

For seven-circular-hoop or seven-spiral reinforcement under weak axis bending (Fig. 5(c)), the DCSS model is the superposition of three DCSS models for single-circular-hoop (Eq. (10)) or single-spiral (Eq. (21)) reinforcement with $l = l$, $l + 0.5D'$, and $l + D'$.

$$V_{s\_l}^{seven\_weak} = 2V_{s\_l}^{one} + 3V_{s\_l+0.5D'}^{one} + 2V_{s\_l+D'}^{one} \tag{24}$$

For seven-circular-hoop or seven-spiral reinforcement under strong axis bending (Fig. 5(d)), the DCSS model is the superposition of five DCSS models for single-circular-hoop (Eq. (10)) or single-spiral (Eq. (21)) reinforcement with, $l = l$, $l + 0.5D'$, $l + D'$, $l + 1.5D'$, and $l + 2D'$.

$$V_{s\_l}^{seven\_strong} = V_{s\_l}^{one} + 2V_{s\_l+0.5D'}^{one} + V_{s\_l+D'}^{one} + 2V_{s\_l+1.5D'}^{one} + V_{s\_l+2D'}^{one} \tag{25}$$

Note that the aforementioned models are applicable to any shear crack location $l$ and any shear crack angle θ.

## NORMALIZED SHEAR STRENGTH FACTOR

To examine the relationship between the proposed DCSS models and the integral averaging method (Eq. (4)), a normalized shear strength factor φ is defined as follows

$$\varphi = \frac{V_s \text{ by DCSS model}}{V_s \text{ by integral averaging method (Eq. (4))}} \tag{26}$$

The φ factor depends on the shear crack location $l$, the shear crack angle θ, the ratio of the vertical spacing to the diameter of a hoop or spiral $s/D'$. For two-circular-hoop and spiral reinforcement, the φ factor also depends on the center-to-center spacing of hoops or spirals $d_{il}$. Note that sinβ in the DCSS models for spiral reinforcement can be expressed as a function of $s/D'$.

$$\sin\beta = \frac{1}{\sqrt{1+(s/2D')^2}} \tag{27}$$

## CRITICAL SHEAR CRACK

The critical shear crack corresponds to the crack that produces the smallest shear strength. To examine the location of the critical shear crack, shear strengths for varying crack locations ($l/D'$) were calculated by each of the proposed DCSS models. Results were expressed using the φ factor. In this section, only the results with a shear crack angle θ of 45 degrees is presented. However, the findings of this section are applicable to other crack angles as well because, as will be shown later, the location of the critical shear crack is independent of θ. Figure 6 shows the relationships between the φ factor and $l/D'$ for representative $s/D'$. All the curves in Fig. 6 oscillate periodically with varying crack locations. Crack locations corresponding to the valleys of the oscillations represent the locations for local critical shear cracks, which produce local minimum values of shear strength. The global minimum value—that is, the smallest shear strength—can be governed by any of the local critical shear cracks. In other words, the critical shear crack can be from any of the local critical shear cracks. Examination of the locations of local critical shear cracks revealed that they correspond to when a shear crack intercepts at least one hoop or spiral edge (independent of θ). Interception at the edge yields no shear strength because $\sin\alpha = 0$ (Eq. (2)). Figure 5 illustrates cases when interception occurs at the edge.

For two-circular-hoop and spiral reinforcement under weak axis bending, there are two cases in which interception occurs at the edge (Fig. 5(a)). Figures 6(a) and 6(b) show the relationships between φ and $l/D'$ for two-circular-hoop and two-spiral reinforcement, respectively. It can be seen that the two cases yield the same local minimum shear strength due to the symmetry of the reinforcement layout. Therefore, the local minimum value is the global minimum value. When, for example, $s/D' = 0.25$ and 0.4 for the two-circular-hoop and two-spiral reinforcement, respectively, the two cases occur at the same value of $l/D'$. This means the critical shear crack intercepts the left and right edges simultaneously, which is illustrated in Fig. 7(a) and 7(c) for two-circular-hoop and two-spiral reinforcement, respectively. This occurs when $D'\cos\theta/s =$ integer for two-circular-hoop reinforcement and $D'\cos\theta/s =$ integer + 0.5 for two-spiral reinforcement. This is the most unfavorable situation for shear strength. When, for example, $s/D' = 0.30$ for both the two-circular-hoop and two-spiral reinforcement, the two cases occur at different values of $l/D'$. This means the critical shear crack does not intercept the left and right edges simultaneously. Three such cases, one case (1) and two cases (2), are illustrated in Fig. 7(b) and 7(d) for two-circular-hoop and two-spiral reinforcement, respectively, to explain why the two cases occur alternately as the shear crack moves along the column.

For two-circular-hoop and spiral reinforcement under strong axis bending, there are four cases in which interception occurs at the edge (Fig. 5(b)). Figures 6(c) and 6(d) illustrate relationships between φ and $l/D'$ for two-circular-hoop and two-spiral reinforcement with $d_{il} = R$, respectively. It can be seen that Cases 1 and 4 yield the same shear strength, as do Cases 2 and 3, due to symmetry of the reinforcement layout. Therefore, to determine the smallest shear strength, it is sufficient to examine only Cases 1 and 2. For two-circular-hoop reinforcement, when, for example $s/D' = 0.25$ (Fig. 6(c)), all the cases occur at the same $l/D'$, which means all the edges are intercepted by the critical shear crack simultaneously (Fig. 8(a)). This leads to a drastic reduction in shear strength and occurs when $D'\cos\theta/s =$ integer and $d_{il}\cos\theta/s =$ integer. When, for example, $s/D' = 0.40$, the four cases occur at different $l/D'$ (Fig. 8(b)). The global minimum is governed by Case 1 (= Case 4). For two-spiral reinforcement, due to the complicated geometry, a shear crack cannot intercept all four edges simultaneously. Figure 8(c) illustrates $s/D' = 0.25$, where Cases 1 and 2 occur at the same $l/D'$, as do Cases 3 and 4. Figure 8(d) illustrates $s/D' = 0.30$, in which the shear crack intercepts only one edge at a time. The smallest shear strength is governed by Case 2 (= Case 3) (Fig. 8(d)).

For seven-circular-hoop and seven-spiral reinforcement under weak axis bending, they do not have the same number of cases in which interception occurs at the edge. Seven-circular-hoop reinforcement has five cases (Cases 1, 2, 3, 4, and 5 in Fig. 5(c)). Seven-spiral reinforcement has one more case (Case 3′ in Fig. 5(c)) because the right edge of the two spirals on the left is not at the same level as the left edge of the two spirals on the right, as illustrated in Fig. 9(a). The case in which the right edge of the two left spirals is intercepted is referred to as Case 3, while the left edge of the two right spirals is intercepted is referred to as Case 3′. Due to symmetry of the reinforcement layout, however, Case 3 yields the same shear strength as Case 3′. Moreover, for both seven-circular-hoop and seven-spiral reinforcement, Cases 1 and 2 yield the same shear strength as Cases 5 and 4, respectively. Therefore, to determine the smallest shear strength, it is sufficient to examine only Cases 1, 2 and 3. Similarly, under strong axis bending, seven-circular-hoop and seven-spiral reinforcement do not have the same number of cases. The former has seven cases (Cases 1, 2, 3, 4, 5, 6, and 7 in Fig. 5(d)), while the latter has three more cases (Cases 3′, 4′, and 5′), as illustrated in Fig. 9(b). For seven-circular-hoop reinforcement, Cases 1, 2, and 3 yield the same shear strength as Cases 7, 6, and 5, respectively. Therefore, only Cases 1, 2, 3, and 4 need to be investigated when determining the smallest shear strength. For seven-spiral reinforcement, due to symmetry, Cases 1, 2, 3, 4, and 5 yield the same shear strength as Cases 7, 6, 5′, 4′, and 3′, respectively. Therefore, to determine the smallest shear strength, Cases 1, 2, 3, 4, and 5, need to be examined.

Figures 6(e) and (f) shows representative relationships between φ and $l/D'$ for seven-circular-hoop and seven spiral reinforcement, respectively, under weak axis bending, and Fig. 6(g) and 6(h) show those under strong axis bending. The relationships are illustrated in Fig. 10 and 11 for under weak and strong axis bending, respectively. In seven-circular-hoop reinforcement, when $D'\cot\theta/s =$ integer×2, all the edges are intercepted by the critical shear crack simultaneously, which does not exist for seven-spiral reinforcement. The complicated geometry of seven-spiral reinforcement due to interlocking of helical shapes avoids interception of all edges by one shear crack and, hence, prevents a drastic reduction in shear strength as seen in seven-circular-hoop reinforcement.

The values of φ in Fig. 6 show that the results of the DCSS models can be higher ($\varphi > 1$) or lower ($\varphi < 1$) than those of the integral averaging method, depending on crack locations

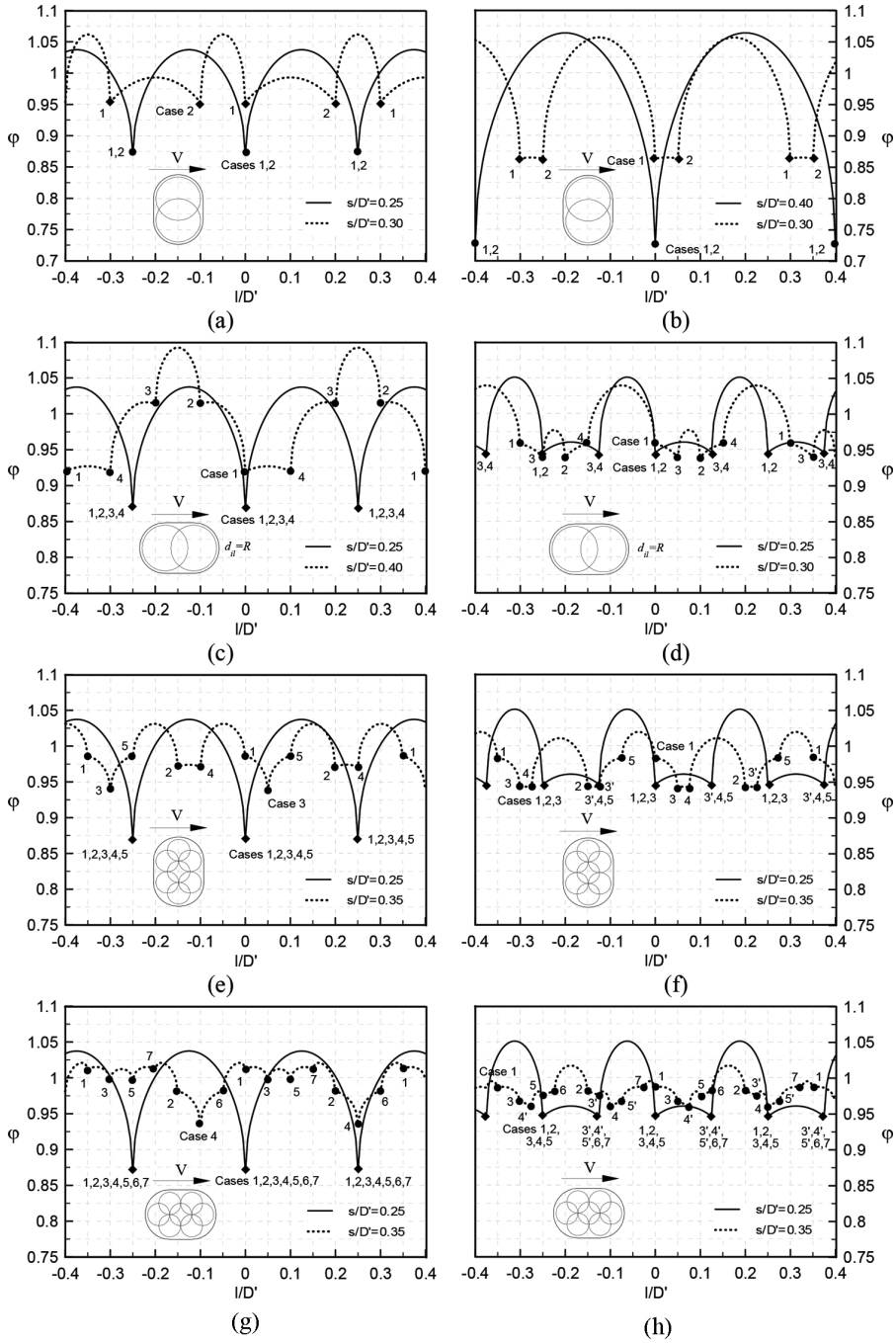


*Fig. 6—Effect of* l/D′ *on φ factor: (a) two-circular-hoop and (b) two-spiral reinforcement under weak axis bending; (c) two-circular-hoop and (d) two-spiral reinforcement under strong axis bending with* $d_{il} = R$*; (e) seven-circular-hoop and (f) seven-spiral reinforcement under weak axis bending; and (g) seven-circular-hoop and (h) seven-spiral reinforcement under strong axis bending.*

($l/D'$). However, the smallest shear strength for a given $s/D'$ by each DCSS model is always lower than that of the integral averaging method.

Based on the above discussion, the DCSS model corresponding to the critical shear crack, referred to as critical DCSS model herein, can be determined by the following equations. For two-circular hoop and spiral reinforcement under weak axis bending, Case 1 ($l = 0$) determines the critical DCSS model. Based on Eq. (22) with $l = 0$

$$V_s^{two\_weak} = 2V_{s\_0}^{one} \tag{28}$$

For two-circular hoop and spiral reinforcement under strong axis bending, the smaller of Cases 1 and 2 ($l = 0$ and $l = -d_{il}$) determines the critical DCSS model. Based on Eq. (23) with $l = 0$ and $l = -d_{il}$

$$V_s^{two\_strong} = \min(V_{s\_0}^{two\_strong}, V_{s\_-d_{il}}^{two\_strong}) \tag{29}$$

For seven-circular hoop and spiral reinforcement under weak axis bending, the smallest of Cases 1, 2, and 3 ($l = 0$, $l = -0.5D'$, and $l = -D'$) determines the critical DCSS model. Based on Eq. (24) with $l = 0$, $l = -0.5D'$, and $l = -D'$

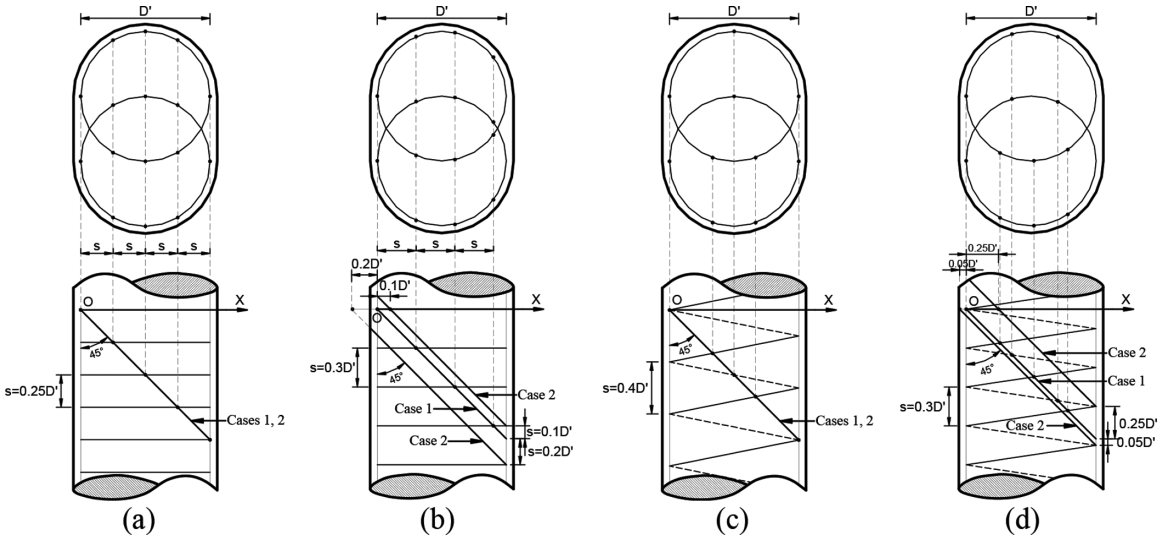


*Fig. 7—Cases when interception occurs at the edge: for two-circular-hoop reinforcement under weak axis bending: (a)* s/D′ *= 0.25, and (b)* s/D′ *= 0.3; and for two-spiral reinforcement under weak axis bending: (c)* s/D′ *= 0.4, and (d)* s/D′ *= 0.3.*

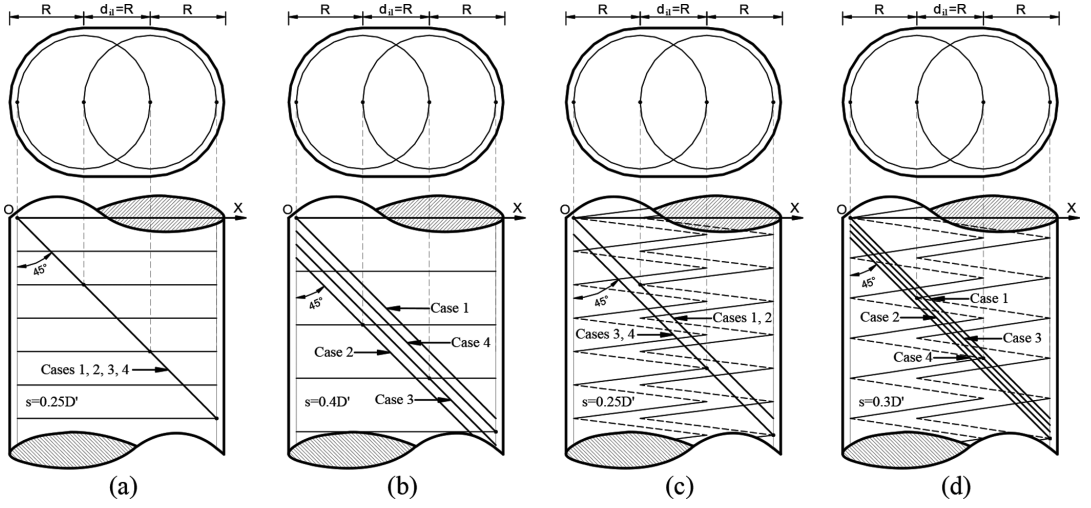


*Fig. 8—Cases when interception occurs at the edge: for two-circular-hoop reinforcement under strong axis bending: (a)* s/D′ *= 0.25, and (b)* s/D′ *= 0.4; and for two-spiral reinforcement under strong axis bending: (c)* s/D′ *= 0.25, and (d)* s/D′ *= 0.3.*

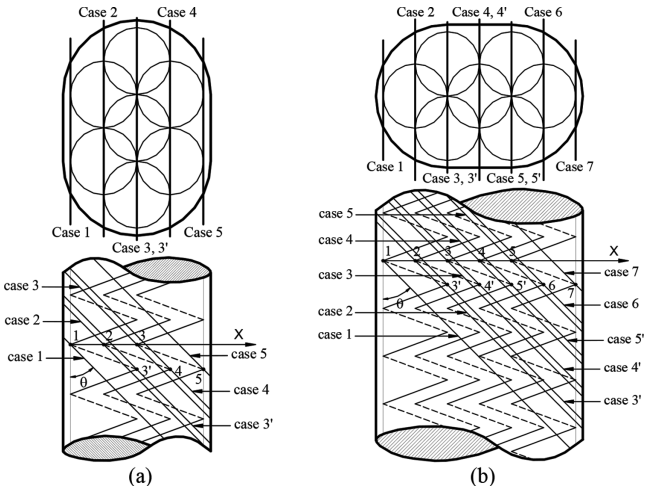


*Fig. 9—Cases when interception occurs at the edge for seven-spiral reinforcement: (a) under weak axis bending; and (b) under strong axis bending.*

$$V_s^{seven\_weak} = \min(V_{s\_0}^{seven\_weak}, V_{s\_-0.5D'}^{seven\_weak}, V_{s\_-D'}^{seven\_weak}) \quad (30)$$

For seven-circular hoop reinforcement under strong axis bending, the smallest of Cases 1, 2, 3, and 4 ($l = 0$, $l = -0.5D'$, $l = -D'$, and $l = -1.5D'$) determines the critical DCSS model. Based on Eq. (25) with $l = 0$, $l = -0.5D'$, $l = -D'$, and $l = -1.5D'$

$$V_s^{seven\_strong} = \min(V_{s\_0}^{seven\_strong}, V_{s\_-0.5D'}^{seven\_strong}, V_{s\_-D'}^{seven\_strong}, V_{s\_-1.5D'}^{seven\_strong}) \quad (31)$$

For seven-spiral reinforcement under strong axis bending, the smallest of Cases 1, 2, 3, 4, and 5 ($l = 0$, $l = -0.5D'$, $l = -D'$, $l = -1.5D'$, and $l = -2D'$) determines the critical DCSS model. Based on Eq. (25) with $l = 0$, $l = -0.5D'$, $l = -D'$, $l = -1.5D'$, and $l = -2D'$

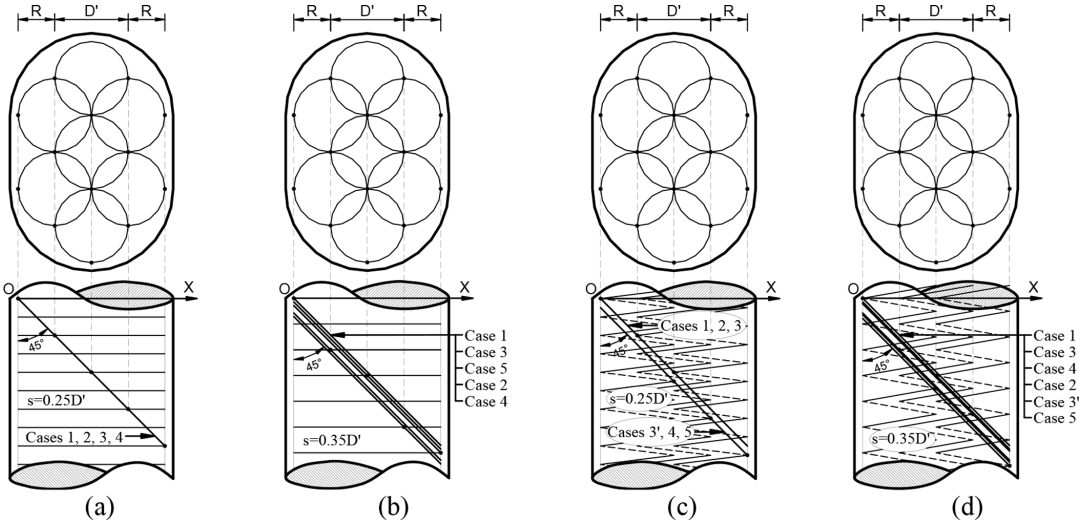


*Fig. 10—Cases when interception occurs at the edge: for seven-circular-hoop reinforcement under weak axis bending: (a)* s/D′ *= 0.25, and (b)* s/D′ *= 0.35; and for seven-spiral reinforcement under weak axis bending: (c)* s/D′ *= 0.25, and (d)* s/D′ *= 0.35.*

$$V_s^{seven\_strong} = \min(V_{s\_0}^{seven\_strong}, V_{s\_-0.5D'}^{seven\_strong}, V_{s\_-D'}^{seven\_strong}, V_{s\_-1.5D'}^{seven\_strong}, V_{s\_-2D'}^{seven\_strong}) \quad (32)$$

## φ FACTOR FOR CRITICAL SHEAR CRACK

With the critical DCSS models (Eq. (28) to (32)), the φ factor for the critical shear crack was calculated for various values of $s/(D'\cot\theta)$. Results are plotted in Fig. 12. For two-circular-hoop and spiral reinforcement, three cases with $d_{il} = R$, $d_{il} = 1.25R$, and $d_{il} = 1.5R$ are presented. Note that the Caltrans BDS[15] requires $d_{il}$ in the range of 1.0 to 1.5 times the radius of the hoop or spiral $R$. For two- and seven-spiral reinforcement, sinβ the part of the φ factor depends only on $s/D'$ (Eq. (27)). Therefore, different values of θ lead to different relationships of φ versus $s/(D'\cot\theta)$. The relationships for θ of 30 and 45 degrees, which cover most practical applications, are plotted in Fig. 12.

All the values of φ in Fig. 12 are less than 1, meaning the shear strength by the critical DCSS models is less than that by the integral averaging method. The φ factor tends to decrease with increasing $s/(D'\cot\theta)$. This means the error of the integral averaging method increases with increasing $s/(D'\cot\theta)$. If 10% probable error is used as a criterion for acceptance of integral averaging, the highest allowable values of $s/(D'\cot\theta)$ are 0.24, 0.24, 0.33, 0.24, 0.24, and 0.24 for two-circular-hoop reinforcement under weak axis bending; two-circular-hoop reinforcement under strong axis bending with $d_{il} = R$, $1.25R$, and $1.5R$; and seven-circular-hoop reinforcement under weak axis bending, and strong axis bending, respectively. Because reinforced concrete columns typically have $\theta \le 45$ degrees, θ can be conservatively taken as 45 degrees. Thus, the highest allowable values of $s/D'$ are 0.24, 0.24, 0.33, 0.24, 0.24, and 0.24, respectively. For two-spiral reinforcement under weak axis bending, two-spiral reinforcement under strong axis bending with $d_{il} = R$, $1.25R$, and $1.5R$, and seven-spiral reinforcement under weak axis bending, and strong axis bending, respectively. Thus, the highest allowable values of $s/(D'\cot\theta)$ are 0.22, 0.39, 0.29, 0.38, 0.39, and 0.43, respectively, with θ of 45 degrees. They are 0.22, 0.33, 0.28, 0.31, 0.33, and 0.33, respectively, for θ of 30 degrees. Again, θ can be conservatively taken as 45 degrees. Therefore, the highest allowable values of $s/D'$ are 0.22, 0.39, 0.29, 0.38, 0.39, and 0.43, respectively. When $s/D'$ is larger than the above values, engineers can either use the critical DCSS models (Eq. (28) to (32)) to calculate shear strength or use the φ factor plots in Fig. 12 to adjust results of the integral averaging method. An example of shear strength calculation for two-spiral reinforcement using the critical DCSS models, φ factor plots, and integral averaging method is given in Appendix A.*

## COMPARISON WITH TEST RESULTS

In Table 1, the test data of two-spiral and seven-spiral columns from earlier studies[2-5,7] are compared with the critical DCSS models and the integral averaging method. The design parameters of the columns are listed in the second to ninth columns of Table 1. The 10th column of Table 1 lists the concrete shear strength for each column calculated based on Caltrans BDS[15] (same as ACI 318[16]), in which the effective shear area is taken as 0.8 gross area of the section. The 11th and 12th columns of Table 1 list the reinforcement shear strength for each column computed by the critical DCSS models $V_{s1}$ and that by the integral averaging method $V_{s2}$, respectively. The shear crack angle is assumed to be 45 degrees according to the codes.[9,10,15,16] The 13th column of Table 1 lists the φ factor ($V_{s1}/V_{s2}$) for each column. The values of the φ factor show that the integral averaging method yields errors ranging from 2% to 16%. Moreover, columns that have an error larger than 10% are those with $s/D'$ larger than the limit presented in the previous section. For instance, Columns 1, 3, and 4 are two-spiral columns subjected to strong axis bending. They have $s/D' = 0.56$—higher than the limit stated in the previous section for such a reinforcement type (0.29 to 0.39), and

*The Appendix is available at **www.concrete.org/publications** in PDF format, appended to the online version of the published paper. It is also available in hard copy from ACI headquarters for a fee equal to the cost of reproduction plus handling at the time of the request.

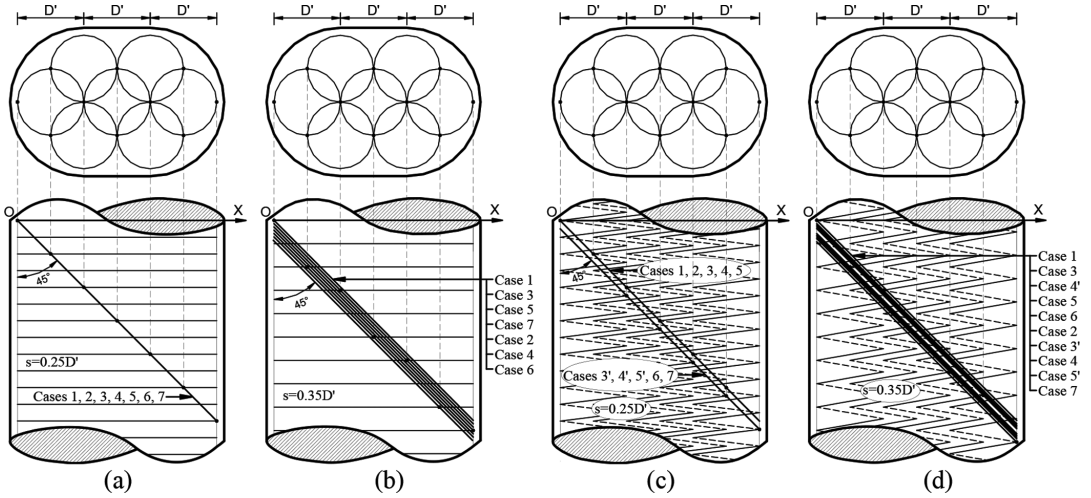


*Fig. 11—Cases when interception occurs at the edge: for seven-circular-hoop reinforcement under strong axis bending: (a)* s/D′ *= 0.25, and (b)* s/D′ *= 0.35; and for seven-spiral reinforcement under strong axis bending: (c)* s/D′ *= 0.25, and (d)* s/D′ *= 0.35.*

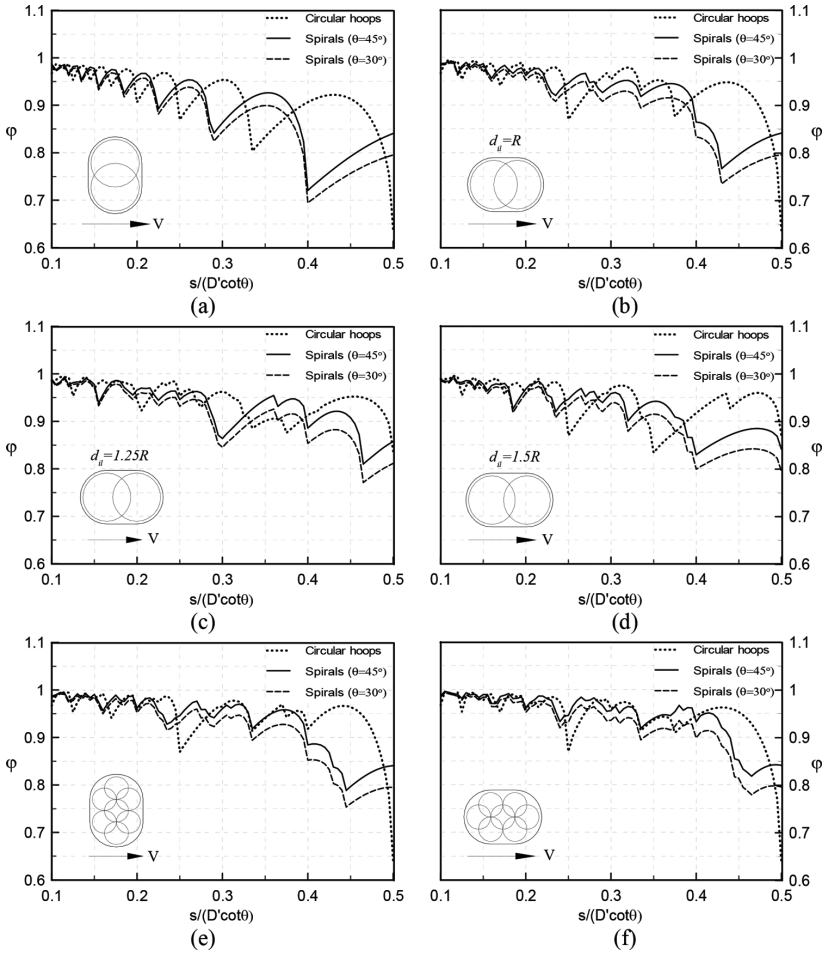


*Fig. 12—Effect of* s/(D′cotθ) *on φ factor: (a) two-circular-hoop and spiral reinforcement under weak axis bending; two-circular-hoop and spiral reinforcement under strong axis bending for (b)* $d_{il}$ = R*, (c)* $d_{il}$ = *1.25*R*, and (d)* $d_{il}$ = *1.5*R*; seven-circular-hoop and spiral reinforcement (e) under weak axis bending, and (f) under strong axis bending.*

show errors of 12 to 14%. Moreover, Column DM2R-SL—a seven-spiral column subjected to strong axis bending—has $s/D'$ = 0.44, which slightly higher than the limit of 0.43. The error of the integral averaging method for this column is 16%. The 17th and 18th columns of Table 1 list the ratio of the measured shear strength to nominal shear strength for each column based on the critical DCSS model $V_{n1}$ and that based on the integral averaging method $V_{n2}$, respectively. Both $V_{n1}$ and $V_{n2}$ are conservative for most of the columns due to the conservative nature of concrete shear strength and

**Table 1—Calculation nominal shear strength of two- and seven-spiral columns and comparison to experimental result**

| Column name | Type | $s/D'$ | $P/A_g f_c'$ | $f_c'$, MPa | $d_t$, mm | $s$, mm | $d_{il}$ (×$R$) | $f_{yh}$, MPa | $V_c$, kN | $V_{s1}$, kN | $V_{s2}$, kN | φ | $V_{N1}$, kN | $V_{N2}$, kN | $V_{max}$, kN | $V_{max}/V_{n1}$ | $V_{max}/V_{n2}$ |
|---|---|---|---|---|---|---|---|---|---|---|---|---|---|---|---|---|---|
| (1) | (2) | (3) | (4) | (5) | (6) | (7) | (8) | (9) | (10) | (11) | (12) | (13) | (14) | (15) | (16) | (17) | (18) |
| 1[2] | Two-S | 0.56 | 0.09 | 32 | 6.35 | 127 | 1.2 | 420* | 77 | 66 | 75 | 0.88 | 143 | 152 | 247 | 1.72 | 1.62 |
| 3[2] | Two-S | 0.56 | 0.09 | 32 | 6.35 | 127 | 1.47 | 420* | 84 | 65 | 75 | 0.86 | 149 | 159 | 275 | 1.85 | 1.73 |
| 4[2] | Two-S | 0.56 | 0.09 | 32 | 6.35 | 127 | 1.2 | 420* | 77 | 66 | 75 | 0.88 | 143 | 152 | 236 | 1.65 | 1.55 |
| Inter 1[3] | Two-S | 0.25 | 0.022 | 35 | 6.35 | 89 | 1.11 | 448 | 183 | 171 | 180 | 0.95 | 354 | 363 | 540 | 1.53 | 1.49 |
| Inter 2[3] | Two-S | 0.25 | -0.1 | 34 | 6.35 | 89 | 1.11 | 448 | 0 | 171 | 180 | 0.95 | 171 | 180 | 414 | 2.42 | 2.30 |
| Inter 3[3] | Two-S | 0.25 | 0.35 | 35 | 6.35 | 89 | 1.11 | 448 | 328 | 171 | 180 | 0.95 | 499 | 508 | 732 | 1.47 | 1.44 |
| Inter 4[3] | Two-S | 0.25 | -0.1 | 37 | 6.35 | 89 | 1.11 | 448 | 0 | 171 | 180 | 0.95 | 171 | 180 | 379 | 2.22 | 2.10 |
| | Two-S | 0.25 | 0.35 | 37 | 6.35 | 89 | 1.11 | 448 | 340 | 171 | 180 | 0.95 | 511 | 521 | 676 | 1.32 | 1.30 |
| 6[4] | Two-S | 0.37 | 0.05 | 31 | 6 | 200 | 0.93 | 364 | 357 | 81 | 87 | 0.93 | 438 | 444 | 529 | 1.21 | 1.19 |
| ISH1.0[5] | Two-S | 0.17 | 0.10 | 34 | 4.05 | 38 | 1.0 | 466 | 77 | 110 | 113 | 0.97 | 187 | 190 | 241 | 1.29 | 1.27 |
| ISH1.25[5] | Two-S | 0.11 | 0.07 | 50 | 4.05 | 25 | 1.25 | 449 | 103 | 163 | 166 | 0.98 | 265 | 268 | 251 | 0.95 | 0.94 |
| ISH1.5[5] | Two-S | 0.11 | 0.08 | 34 | 4.05 | 25 | 1.25 | 467 | 87 | 165 | 172 | 0.96 | 253 | 260 | 253 | 1.00 | 0.97 |
| DM1R-SL[7] | Two-S | 0.22 | 0.06 | 64 | 10 | 120 | 1.0 | 605 | 611 | 628 | 672 | 0.93 | 1239 | 1283 | 1787 | 1.44 | 1.39 |
| DM1R-SS[7] | Two-W | 0.19 | 0.06 | 70 | 10 | 100 | 1.0 | 605 | 640 | 746 | 806 | 0.93 | 1386 | 1446 | 1833 | 1.32 | 1.27 |
| DM2R-SL[7] | Seven-S | 0.44 | 0.07 | 58 | 8 | 120 | NA | 648 | 583 | 679 | 806 | 0.84 | 1262 | 1389 | 1722 | 1.36 | 1.24 |
| DM2R-SS[7] | Seven-W | 0.37 | 0.06 | 69 | 8 | 100 | NA | 648 | 635 | 911 | 967 | 0.94 | 1546 | 1602 | 1744 | 1.13 | 1.09 |
| DM2RI-SS[7] | Seven-W | 0.30 | 0.07 | 55 | 8 | 80 | NA | 648 | 565 | 1134 | 1209 | 0.94 | 1699 | 1774 | 1734 | 1.02 | 0.98 |

*Specified yield strength of transverse reinforcement.

Notes: 1 MPa = 145 psi; 1 mm = 0.0394 in.; 1 kN = 0.225 kip.

the conservative assumption of a crack angle of 45 degrees. $V_{n2}$ is less conservative than $V_{n1}$ because integral averaging overestimates the reinforcement shear strength. The $V_{n1}$ is unconservative for Column ISH1.25, and $V_{n2}$ is unconservative for Columns ISH1.25, ISH1.5, and DM2RI-SS. Note that even though these three columns failed in shear, they showed ductility capacities greater than 4.0, which is expected to greatly reduce the shear strength of the columns.

## CONCLUSIONS

DCSS models were developed in this study for two-circular-hoop and two-spiral transverse reinforcement, and seven-circular-hoop and seven-spiral transverse reinforcement for reinforced concrete columns. With the developed models, critical shear crack locations and relationships between the critical DCSS models and the integral averaging method were examined. Important conclusions are summarized as follows.

1. The DCSS models show that the reinforcement shear strength varies periodically as a shear crack moves along the column. When a shear crack intercepts the edge of at least one hoop series or spiral, local minimum shear strength occurs. The critical shear crack that yields the smallest shear strength (global minimum value) can be from any of the cases in which interception occurs at the edge. There are one, two, three, four, and five such cases that need to be examined to determine the smallest shear strength for two-circular hoop and spiral reinforcement under weak axis bending, and under strong axis bending, seven-circular hoop and spiral reinforcement under weak axis bending, seven-circular hoop reinforcement under strong axis bending, and seven-spiral reinforcement under strong axis bending, respectively.

2. All the left and right edges of hoop series or spirals are intercepted simultaneously by the critical shear crack, when $D'\cot\theta/s$ = integer for two-circular-hoop reinforcement under weak axis bending, $D'\cot\theta/s$ = integer+0.5 for two-spiral reinforcement under weak axis bending, $D'\cot\theta/s$ = integer and $d_{il}\cot\theta/s$ = integer for two-circular-hoop reinforcement under strong axis bending, and $D'\cot\theta/s$ = integer×2 for seven-circular-hoop reinforcement. This can cause a drastic reduction in shear strength and should be avoided in design. The critical shear crack does not intercept all edges simultaneously for two-spiral reinforcement under strong axis bending and for seven-spiral reinforcement due to more complicated reinforcement geometries.

3. The critical DCSS models give lower values of shear strength than the integral averaging method. If 10% probable error is the criterion for acceptance of the integral averaging method, the highest allowable values of $s/D'$ are 0.24, 0.24, 0.33, 0.24, 0.24, and 0.24 for two-circular-hoop reinforcement under weak axis bending, two-circular-hoop reinforcement under strong axis bending with $d_{il} = R$, 1.25$R$, and 1.5$R$, and seven-circular-hoop reinforcement under weak axis bending, and strong axis bending, respectively. The highest allowable values of $s/D'$ are 0.22, 0.39, 0.29, 0.38, 0.39, and 0.43 for two-spiral reinforcement under weak axis bending, two-spiral reinforcement under strong axis bending with $d_{il} = R$, 1.25$R$, and 1.5$R$, and seven-spiral reinforcement under weak axis bending, and strong axis bending, respectively. If $s/D'$ is larger than the above values, the critical

DCSS models or φ factor plots developed in this study can be used to calculate shear reinforcement strength.

4. Comparison with the test results of shear-critical columns from earlier studies shows that both the nominal shear strength based on the critical DCSS models ($V_{n1}$) and that based on the integral averaging method ($V_{n2}$) are conservative for most of the columns. $V_{n2}$ is less conservative than $V_{n1}$ because integral averaging overestimates the reinforcement shear strength.

## AUTHOR BIOS

**Yu-Chen Ou** *is a Professor of civil and construction engineering at National Taiwan University of Science and Technology, Taipei, Taiwan. He received his PhD from the State University of New York at Buffalo, Buffalo, NY. His research interests include reinforced concrete structures and earthquake engineering. He is the Vice President of the Taiwan Chapter – ACI.*

**Si-Huy Ngo** *is a Lecturer of civil engineering at Hong Duc University, Thanhhoa, Vietnam. He received his MS and PhD from National Taiwan University of Science and Technology. His research interests include reinforced concrete structures and prefabrication construction technology.*

## ACKNOWLEDGMENTS

The authors would like to thank the Excellence Research Program of National Taiwan University of Science and Technology for financial support. Former master's student T. N. Khoa is commended for his valuable discussion.

## NOTATION

$A_g$ = gross area of section
$A_{sh}$ = cross-sectional area of transverse reinforcing bar
$A_v$ = total area of shear reinforcement
$a_1$ = coefficient = $\cot\theta - s/2D'$
$a_2$ = coefficient = $\cot\theta + s/2D'$
$b$ = coefficient = $l/2D'$
$D'$ = diameter of circular hoop or spiral
$d_{il}$ = center-to-center spacing of two-circular hoop or two-spiral reinforcement
$d_t$ = diameter of transverse reinforcing bar
$f_c'$ = concrete compressive strength
$f_{yh}$ = yield strength of transverse reinforcement
$i$ = an integer, numbering levels of hoop series or spiral
$l$ = distance from origin of coordinate system to hoop or spiral edge
$N$ = $D'\cot\theta/s$ = ratio of projection of shear crack along Y-axis to spacing of hoops
$n$ = number of circular-hoop series or spirals
$P$ = axial force (positive for compression)
$R$ = $0.5D'$ = radius of circular hoop or spiral
$s$ = spacing of transverse reinforcement
$T_{si}$ = shear resistance provided from $i$-th level of circular-hoop series or spiral
$V_c$ = shear strength provided by concrete
$V_{max}$ = maximum lateral force obtained from experiment
$V_{n1}$ = nominal shear strength based on critical DCSS models
$V_{n2}$ = nominal shear strength based on integral averaging method (Eq. (4))
$V_s$ = shear strength provided by shear reinforcement
$V_{s1}$ = shear reinforcement strength computed by critical DCSS models
$V_{s2}$ = shear reinforcement strength computed by integral averaging method (Eq. (4))
$V_{s\_l}^{one}$ = shear strength provided by single hoop or spiral reinforcement for shear crack location
$V_s^{seven\_strong}$ = critical shear strength provided by seven-circular-hoop or seven-spiral reinforcement under strong axis bending
$V_{s\_l}^{seven\_strong}$ = shear strength provided by seven-circular-hoop or seven-spiral reinforcement under strong axis bending for shear crack location $l$
$V_s^{seven\_weak}$ = critical shear strength provided by seven-circular-hoop or seven-spiral reinforcement under weak axis bending
$V_{s\_l}^{seven\_weak}$ = shear strength provided by seven-circular-hoop or seven-spiral reinforcement under weak axis bending for shear crack location $l$
$V_s^{two\_strong}$ = critical shear strength provided by two-circular-hoop or two-spiral reinforcement under strong axis bending
$V_{s\_l}^{two\_strong}$ = shear strength provided by two-circular-hoop or two-spiral reinforcement under strong axis bending for shear crack location $l$
$V_s^{two\_weak}$ = critical shear strength provided by two-circular-hoop or two-spiral reinforcement under weak axis bending
$V_{s\_l}^{two\_weak}$ = shear strength provided by two-circular-hoop or two-spiral reinforcement under weak axis bending for shear crack location $l$
$x$ = x-coordinate of Cartesian coordinate system
$x_i$ = x-coordinate of intersection of shear crack and $i$-th hoop or spiral
$y$ = y-coordinate of Cartesian coordinate system
$\alpha_i$ = angle between horizontal and line from center of spiral or circular hoop to point intersected by shear crack for $i$-th intersection
$\alpha_i^1$ = $\alpha_i$ for back side of hoop or spiral (Fig. 2).
$\alpha_i^2$ = $\alpha_i$ for front side of hoop or spiral (Fig. 2).
$\beta$ = angle between transverse reinforcement and longitudinal axis of column
$\varphi$ = ratio between shear reinforcement strength calculated by DCSS models and by integral averaging method (Eq. (4))
$\theta$ = angle between shear crack and longitudinal axis of column

## REFERENCES

1. Tanaka, H., and Park, R., "Seismic Design and Behavior of Reinforced Concrete Columns with Interlocking Spirals," *ACI Structural Journal*, V. 90, No. 2, Mar.-Apr. 1993, pp. 192-203.

2. McLean, D. I., and Buckingham, G. C., "Seismic Performance of Bridge Columns with Interlocking Spiral Reinforcement." *Report* No. WA-RD 357.1, Washington State Transportation Center, Seattle, WA, 1994, 41 pp.

3. Benzoni, G.; Priestley, M. J. N.; and Seible, F., "Seismic Shear Strength of Columns with Interlocking Spiral Reinforcement," 12th World Conference on Earthquake Engineering, Auckland, New Zealand, 2000, 8 pp.

4. Igase, Y.; Nomura, K.; Kuroiwa, T.; and Miyagi, T., "Seismic Performance and Construction Method of Bridge Columns with Interlocking Spiral/Hoop Reinforcement," *Concrete Journal*, V. 40, No. 2, 2002, pp. 37-46. doi: (in Japanese)10.3151/coj1975.40.2_37

5. Correal, J. F.; Saiidi, M. S.; Sanders, D.; and El-Azazy, S., "Shake Table Studies of Bridge Columns with Double Interlocking Spirals," *ACI Structural Journal*, V. 104, No. 4, July-Aug. 2007, pp. 393-401.

6. Wu, T.-L.; Ou, Y.-C.; Yin, S. Y. L.; Wang, J.-C.; Wang, P.-H.; and Ngo, S.-H., "Behavior of Oblong and Rectangular Bridge Columns with Conventional Tie and Multi-spiral Transverse Reinforcement under Combined Axial and Flexural Loads," *Journal of the Chinese Institute of Engineers*, V. 36, No. 8, 2013, pp. 980-993. doi: 10.1080/02533839.2012.747047

7. Ou, Y. C.; Ngo, S. H.; Yin, S. Y.; Wang, J. C.; and Wang, P. H., "Shear Behavior of Oblong Bridge Columns with Innovative Seven-Spiral Transverse Reinforcement," *ACI Structural Journal*, V. 111, No. 6, Nov.-Dec. 2014, pp. 1339-1349. doi: 10.14359/51686873

8. Ou, Y. C.; Ngo, S. H.; Roh, H.; Yin, S. Y.; Wang, J. C.; and Wang, P. H., "Seismic Performance of Concrete Columns with Innovative Seven- and Eleven-Spiral Reinforcement," *ACI Structural Journal*, V. 112, No. 5, Sept.-Oct. 2015, pp. 579-592. doi: 10.14359/51687706

9. California Department of Transportation, "Seismic Design Criteria Version 1.6," Engineering Service Center, Earthquake Engineering Branch, Nov. 2010, 160 pp.

10. American Association of State Highway and Transportation Officials, "AASHTO Guide Specifications for LRFD Seismic Bridge Design," second edition, Washington, DC, 2011, 296 pp.

11. Ang, B. G.; Priestley, M. J. N.; and Paulay, T., "Seismic Shear Strength of Circular Reinforced Concrete Columns," *ACI Structural Journal*, V. 86, No. 1, Jan.-Feb. 1989, pp. 45-59.

12. Dancygier, A. N., "Shear Carried by Transverse Reinforcement in Circular RC Elements," *Journal of Structural Engineering*, ASCE, V. 127, No. 1, 2001, pp. 81-83. doi: 10.1061/(ASCE)0733-9445(2001)127:1(81)

13. Kim, J. H., and Mander, J. B., "Theoretical Shear Strength of Concrete Columns Due to Transverse Steel," *Journal of Structural Engineering*, ASCE, V. 131, No. 1, 2005, pp. 197-199. doi: 10.1061/(ASCE)0733-9445(2005)131:1(197)

14. Jaafar, K., "Discrete Versus Average Integration in Shear Assessment of Spiral Links," *Canadian Journal of Civil Engineering*, V. 36, No. 2, Feb. 2009, pp. 171-179. doi: 10.1139/L08-106

15. California Department of Transportation, "Bridge Design Specifications," Engineering Service Center, Earthquake Engineering Branch, Sacramento, CA, Sept. 2003, pp. 8-1 to 8-58.

16. ACI Committee 318, "Building Code Requirements for Structural Concrete (ACI 318-11) and Commentary," American Concrete Institute, Farmington Hills, MI, 2011, 503 pp.